Renewable Energy 146 (2020) 9–15

Contents lists available at ScienceDirect

Renewable Energy

journal homepage: www.elsevier.com/locate/renene

Dynamic wake steering and its impact on wind farm power production and yaw actuator duty☆

Stoyan Kanev*

TNO, ECN Wind Energy, Westerduinweg 3, 1755LE, Petten, the Netherlands

ARTICLE INFO

Article history:
Received 5 November 2018
Received in revised form
7 May 2019
Accepted 21 June 2019
Available online 25 June 2019

Keywords:
Wind farm control
Wake redirection
Dynamic adaptation
Yaw actuator duty cycle

ABSTRACT

Wake redirection is a wind farm control strategy that aims at increasing the overall power yield of a wind farm. It involves intentional misalignment of the rotors of upstream wind turbines with respect to the wind direction, thereby diverting their wakes aside from downstream turbines. The yaw misalignment angles are typically optimized using static wake models. In real-life, due to the rapid fluctuations of the wind direction with time, the optimized yaw misalignment angles cannot be instantaneously tracked as this would inevitably require an unacceptable amount of rotor yawing. This work is focused on how to dynamically adapt the statically optimzied yaw misalignment angles to achieve a good balance between high energy gain and limited yaw actuator duty cycle.

1. Introduction

Active Wake Control (AWC) is a strategy for operating wind farms in a cooperative manner in order to reduce wake effects as to maximize the overall power production of the wind farm and/or reduce the loading on the individual wind turbines [1,2]. There exist two main classes of AWC algorithms. The first one, called induction control, relies on down-regulation of upstream wind turbines to effectively decrease their axial induction, thereby letting the turbines in their wakes to benefit from increased wind velocity [3–6]. Rather than reducing the wake deficit, the second approach, called wake redirection, aims to steer the wakes away from downstream wind turbines by operating the upstream turbines with yaw misalignment [7–9]. Wake redirection is typically the more beneficial strategy in terms of power production increase potential. As such, it has received a lot of attention recently by the research community, focused on topics ranging from modeling the effects from yaw misalignment [10,11], to including loads into the optimization [12,13], to using flow-measurements in a feedback control setting [14]. Recently, NREL published the first measurement results from test with wake redirection on a few offshore wind turbines [15]. For a more detailed view on the impacts of the two AWC strategies on the power production and fatigue loads for different existing wind farms, the reader is referred to Ref. [13].

The current approach to determine the yaw misalignment angles that optimize the benefits from wake redirection is static and results in a lookup table (LUT). This LUT contains the optimal yaw offsets for each turbine in the farm, each wind direction (and possibly wind speed) bin, and depending on the site conditions possibly also variables such as atmospheric stability. Computing a LUT that maximizes the annual energy production (AEP) of the wind farm is therefore a complex, non-linear multidimensional optimization problem. Recent studies for different wind farms indicate that there is a significant potential for AEP increase by wake redirection [9,13]. However, these studies are based on a static analysis where the potential power gains are determined by evaluating a range of constant wind conditions. Clearly, such static simulations disregard the very slow dynamics of the turbine yaw system. Due to the very slow yaw dynamics, the nacelle is not capable of accurately tracking the rapidly changing yaw setpoints from the LUT that are driven by the fast variations in the wind direction, which currently forms the main challenge for practical application of AWC. During normal operation, the rotor orientation is dynamically controlled to achieve a good balance between maximizing the power production (requiring increased level of yawing) and minimizing the loads on the yaw system (requiring limited yaw motion). While the impact on loads on other components of the wind turbines (blades, shaft, tower, etc.) are at least

☆ This work has received funding from the European Union's Horizon 2020 research and innovation programme under grant agreement No 727477 (CL-Windcon project).

* Corresponding author.
E-mail address: stoyan.kanev@tno.nl.

https://doi.org/10.1016/j.renene.2019.06.122
0960-1481/

equally important, these have recently been studied in much detail for several existing wind farms and are already quite well understood [13]. There, however, the impact on the turbine yawing is not considered, which is the focus of this paper. Under wake redirection, optimizing this balance properly is even more important due to the high sensitivity of the yaw misalignment angle to wind direction changes; just a small change in the wind direction by a few degrees may require the rotor orientation to be modified from a large positive to a large negative angle - an action that would typically take minutes to complete.

The contribution of this paper is to provide a guideline for how to arrive at an optimal dynamic yaw adaptation strategy. To this end, a dynamic adaptation algorithm is considered, consisting of a low-pass filter, sample and hold mechanism, and hysteresis. For the parameters of these three building blocks, a range of realistic values is selected and time domain simulations are performed using wind series measured at a real-life metmast. The results from this sensitivity study allows to select the best set of parameters of the adaptation algorithm in terms of desired balance between energy gain and yaw duty.

2. Wind farm control by wake redirection

Wake redirection is an approach to control the wakes in a wind farm, which is based on yaw misalignment, i.e. yawing the rotors of the upstream wind turbines away from the wind. As a result of that, two things happen: the power production of the yawed wind turbines decreases because the effective rotor area affected by the incoming wind flow becomes smaller, and the wakes behind these turbines is redirected aside from the downstream wind turbines (see Fig. 1). Due to the fact that the wake is being diverted, the downstream turbines can get (a larger portion of) the undisturbed wind field, which increases their power production.

Numerous simulation studies with wake redirection indicate the large potential for energy increase [16,17]: even for a row of just 3 turbines, an energy yield increase of more than 10% can be realized by wake redirection. For long rows containing many wind turbines, this gain in energy can even reach up to 30%! Recently, tunnel tests [6] and field tests [15] confirm that the technology can be very beneficial for reducing wake effects on the power production.

2.1. Static optimization

The purpose of AWC is to operate the wind farm so as to increase the economical benefit over the lifetime. This, however, is influenced by many factors, such as the power curve, the wind resource, the operation and maintenance (O&M) costs, turbine availability, power limitations imposed by the transmission system operator, etc. The AWC farm operation strategy has influence on the power production of the farm and on the fatigue loads of the wind turbines. The loads, in turn, are related to the O&M costs. However, since at present there are no well-established models of the relationship between loads and O&M costs, maximization of the AEP of the wind farm is chosen here as optimization criterion.

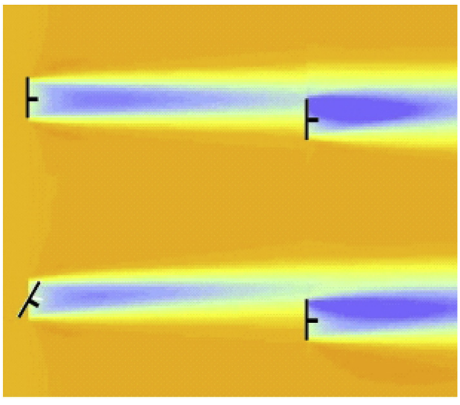

Fig. 1. Visualization of the effect from wake redirection on the wake (bottom) as compared to the nominal situation (top).

The optimal yaw misalignment settings clearly strongly depend on the wind direction as that defines the location of the wake behind a turbine and the corresponding impact on other turbines behind it. However, there are many other contributors to the wake deficit (and hence the power productions) downstream, such as the wind velocity and the turbulence intensity. Hence, the yaw misalignment offsets should be optimized for all possible variations in the wind conditions expected at a given site. Due to the high computational complexity, it is at present prohibitive to perform the optimization of the yaw misalignments online based on the actually measured wind conditions. Instead, the optimization is performed off-line for a set of wind conditions, resulting into a static multidimensional LUT. More specifically, the yaw misalignment setpoint for each individual wind turbine in the farm are optimized for every combination of wind speed and wind direction. To this end, a wake model is required (see Section 3 for information on the model used in this study), as well as an optimization procedure that, for a fixed wind speed and wind direction, simulates the wind farm with different candidate yaw misalignment setpoints until it converges to the optimal solution in terms of maximal power production of the wind farm. For practical reasons, this optimization would then be performed for a discrete set of wind directions in the interval [0,360) degree (e.g. binned at 1°) and wind speeds between cut-in and rated (also binned at 1 m/s, for instance). The yaw misalignment settings, optimized in this yaw, will be stored in a large 3D LUT with dimensions (turbine number, wind direction, wind speed). For more details on the optimization algorithm, the reader is referred to Ref. [13].

It needs to be pointed out that, due to its static nature of the off-line optimization, the result will only provide an upper limit on the achievable power increase by AWC in real-life. For a realistic prediction of the achievable performance, dynamic simulations are required, which is the focus of this paper.

2.2. Dynamic adaptation algorithm

Since the wind turbine rotor with its very slow dynamics is not capable of following the rapidly changing wind direction, the statically optimized LUT may be suboptimal under time-varying wind conditions. An improvement is expected when the variability of the incoming wind conditions is included into the optimization as uncertainty, e.g. by using the expected probability distribution of the wind direction (and wind speed) for a fixed yaw orientation. However, this probability distribution depends not only on the variability of the wind, but also on the dynamics of the yaw system (i.e. on how fast the nacelle direction will be adapted to track the desired orientation) and even on the LUT itself (as it modofies the dependency of the nacelle orientation on the measured wind direction).

Rather than trying to model and incorporate the uncertainty in the wind conditions into the optimization for the LUT, this paper focuses onto the dynamic adaptation of the yaw misalignemt setpoints using the measured wind conditions. In other words, as the wind conditions within the wind farm vary significantly in time and in space, their local measurements (or estimations) at turbine level will need to be processed before the corresponding yaw

misalignment setpoints are interpolated from the optimized LUT. The goal of the pursued dynamic adaptation strategy is to achieve a good balance between maximizing the power production (requiring increased level of yawing) and minimizing the loads on the yaw system (requiring limited yaw motion). To this end, a structure for the dynamic adaptation algorithm is first selected, consisting of the following three building blocks (see Fig. 2):

- lowpass (LP) filter: a second-order lowpass elliptic filter with 20 dB reduction and 1 dB ripple. It's bandwidth will be varied to study its impact on the performance of the dynamic adaptation algorithm.
- sample-and-hold (sampling): defines the sample time at which the yaw misalignment setpoints will be updated. This sample time will be varied as well.
- hysteresis: this block is included in an attempt to avoid that the yaw misalignment setpoints change sign too often when the wind direction varies around the row orientation, as these require a long yawing motions. Here, the activation/deactivation bounds will be varied.

Notice in Fig. 2 that the first two blocks (LP filter and sampling) are applied on both the wind speed and wind direction signals, while the Hysteresis block only works on the wind direction signal. Notice that the wind direction signal is not directly measured, but computed using measurements of the nacelle direction and the yaw error. The forth block in the figure represents the static LUT containing the optimized yaw misalignment setpoints. Finally, the last block in Fig. 2 depicts the wind turbine yaw control system that yaws the nacelle to control the yaw error. It should also be pointed out that each wind turbine can use its own measurements and have its own implementation of the AWC algorithm in Fig. 2, therefore being independent on the measurements performed at other turbines (decentralized AWC). Alternatively, the local measurements at the individual wind turbines can be collected at a central level (centralized AWC implemented in a farm controller), processed to obtain one single representative wind speed and direction for the whole farm, therefore having the AWC algorithm implemented at farm level. Other, intermediate, implementations are, of course, also possible. While the approach discussed in this paper allows for any of this options, in the simulation study presented later on the centralized implementation is used.

3. Results and discussion

To study the impact of the considered parameters of the dynamic adaptation algorithm on its performance in terms of power gain and yaw duty, a sensitivity study is performed. A simple fictive wind farm is considered, simulated under reaslistic wind conditions as measured by a real-life metmast at ECN test site Wieringermeer. The time-series for the wind speed and wind direction signal used in the simulations are given in Fig. 3, and consist of 300 min of 10 s averaged measurements (10 s being also the sample time of the simulations). Notice that the wind direction series simulated varies around 90°, representing Eastern winds. The farm layout is regular, consisting of 3 rows of 3 turbines each, the rows being aligned with the North-South and East-West directions. The distances between the turbines is 5D (North to South) and 7D (East to West). This wind farm is defined as one of the reference wind farms in the CL-Windcon project. The reference wind turbine model, defied in that project and used in this study, is the DTU 10 MW reference wind turbine [18], which has a rotor diameter of 178.3 m.

The LUT containing the yaw misalignment setpoints has been optimized using the FarmFlow wake model, a simplified 3D CFD model [19,20]. Even though in this study the LUT is only optimized with respect to the wind direction, this is not a significant limitation as the sensitivity of the yaw angles to the wind velocity is typically very weak anyway. Nevertheless, even though independent on the wind velocity, the misalignment angles are optimized with respect to the power production for the range of wind speeds between 4 and 13 m/s by using the wind speed distribution (Weibull distribution with shape parameter $k = 2$ and scale parameter $A = 10$). The optimized yaw misalignment settings for the turbine at the South-East corner (denoted as T7 in the sequel) are given in the left-hand side plot in Fig. 4. Besides the optimized yaw angles (dashed line), the plot depicts a Bezier curve approximation of these (solid curve) which is applied to smoothen the optimal curve. At the right-hand side of Fig. 4, a plot is provided giving the static relative increase of the power production of the wind farm, for a single wind speed (8 m/s) and a sector of wind directions, as computed by the FarmFlow and FLORIS wake models [16].

The time-domain simulations are performed using the wake model FLORIS, extended with a time-delay model to account for the dynamics of the propagation of wind speed and wind direction changes throughout the wind farm. The time delays depend on the 10-min average wind velocity and the downstream distances between the turbines, calculated using the 10-min average wind direction.

First, a nominal simulation is performed without wake redirection to serve as a basis for comparison. Subsequently, a series of simulations is performed with wake redirection using different parameters of the dynamic adaptation strategy outlined in Section 2.2. The following parameter variations are considered (see Fig. 2):

- The AWC sample time at which the yaw misalignment settings are updated: 10, 20, 30, 60, 120, 300, 600 s.
- The LP filter time constant: 10, 20, 30, 60, 120, 300, 600 s.
- four cases are considered for the activation and deactivation bounds of the hysteresis block: $\mathscr{H}_{(0,0)}$ (no hysteresis), $\mathscr{H}_{(0.5,1)}$, $\mathscr{H}_{(1,2)}$, $\mathscr{H}_{(-1,1)}$, $\mathscr{H}_{(-2,2)}$, where $\mathscr{H}_{(x,y)}$ denotes the following hysteresis logic (see Fig. 5):

$$w_{d,hyst}(k) = \begin{cases} w_d(k), & \text{if } w_d(k) \geq 90+y \text{ OR } w_d(k) \leq 90-y \\ 90\,\text{deg}, & \text{if } w_d(k) < 90+x \text{ AND } w_d(k) > 90-x \\ w_{d,hyst}(k-1), & \text{otherwise} \end{cases}$$

Here, $w_d(k)$ denotes the input (i.e. wind direction at time instant k) and $w_{d,hyst}(k)$ – the output of the hysteresis. Notice that the hysteresis is centred at 90° (see also Fig. 4).

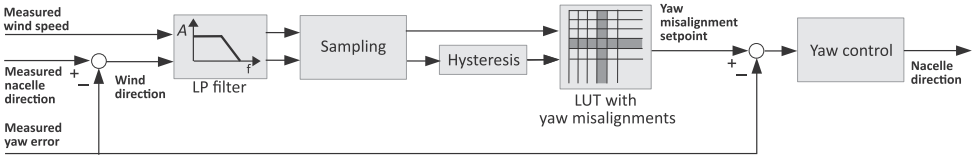

Fig. 2. Block diagram of the AWC dynamic adaptation algorithm.

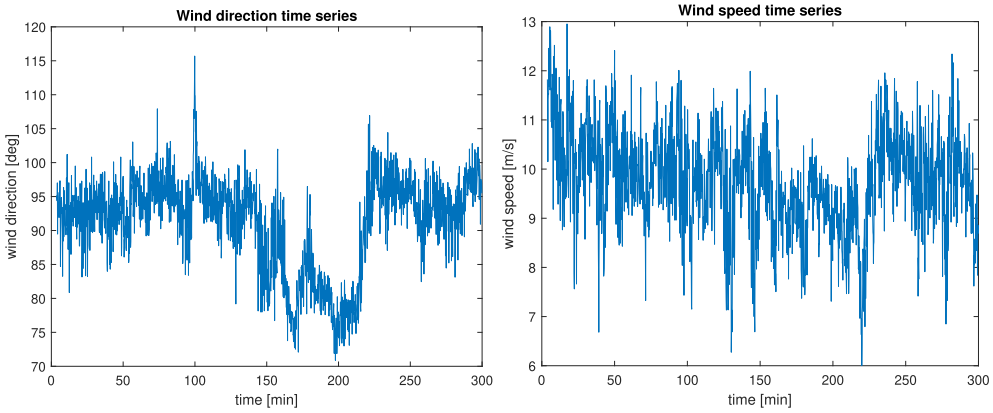

Fig. 3. Wind direction (left) and wind speed (right) time-series used in the performed simulations.

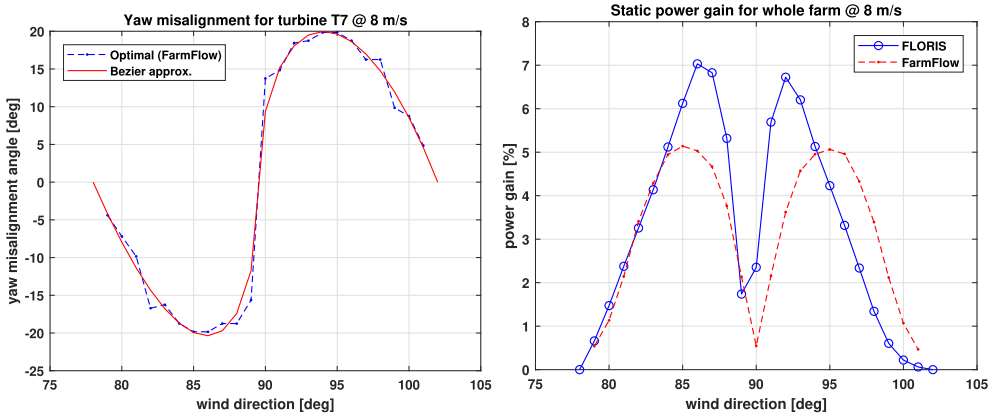

Fig. 4. Yaw misalignment angles for turbine T7 (left), and static power production gain for the whole farm (right) as function of the wind direction.

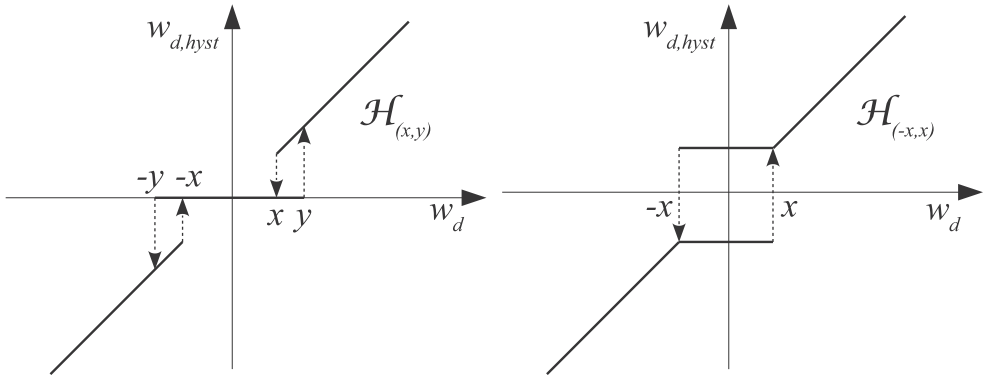

Fig. 5. Hysteresis types considered in the study: $\mathscr{H}_{(x,y)}$ (left) and $\mathscr{H}_{(-x,x)}$ (right).

As an example of the time-domain result of one simulation, Fig. 6 is provided. The figure depicts the performance of the yaw control algorithm that aims, under normal operation, at directing the nacelle (black/dark thick curve) towards the wind (blue/dark thin curve). As it can be seen, the nominal yaw control algorithm is not too aggressive, tracking pretty well the slower changes in the wind direction. Notice also that due to the inability of the nacelle to keep track with the fast changes in the wind direction, the rotor will regularly operate at some misalignment with respect to the wind direction. The nacelle direction is also plotted for the case with wake redirection control active without hysteresis (magenta/light thin curve) and with $\mathscr{H}_{(-2,2)}$ hysteresis (cyan/light thick curve). In this specific simulation, AWC sample time is 120s, and LP filter time constant is 300s. It can clearly be seen that adding hysteresis reduces the yaw travel as expected.

The results from the complete series of simulations are summarized graphically in Figs. 7–9. The left plot in Fig. 7 depicts the wind farm energy gain as function of the AWC sample time and LP filter time constant, with hysteresis not applied. The plane on the top (labelled “static” in the legend) represents the theoretical energy gain that is achieved for the selected wind series based on static simulations with the yaw misalignment angles directly

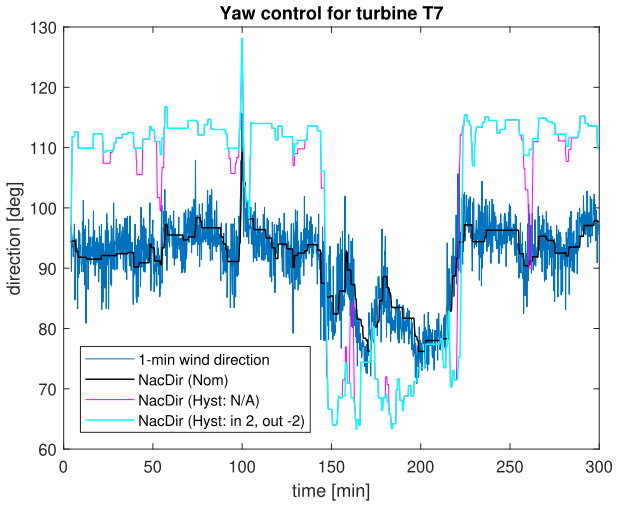

Fig. 6. Simulation result for the nacelle direction of turbine T7 without (dark/black thick line) and with (light/cyan thick line) wake redirection control. (For interpretation of the references to colour in this figure legend, the reader is referred to the Web version of this article.)

interpolated from the LUT using the unprocessed wind direction (i.e. the blue line in Fig. 6) without any dynamic adaptation. This idealistic gain serves as an upper limit on the achievable energy gain, as it is based on the unrealistic assumption that the nacelle direction can follow the optimal yaw setpoints instantaneously. The surface below that represents the results from the dynamic simulations. For instance, the results from the time domain simulation, plotted in Fig. 6, have been performed with AWC sample time of 120s and LP filter time constant of 300 s (and without hysteresis), so that the corresponding energy gain can be read from Fig. 7 as being 2.14%. From this plot it can be concluded that the potential energy gain that gets lost when dynamics are included is roughly in the range of $1/4$ to $1/3$ of the ideal static gain. Furthermore, the sensitivity of the energy gain on the AWC sample time is clearly much more pronounced than that on the LP filter time constant. In terms of energy gain, best results are achieved for AWC sample times up to 120 s, provided that the LP filter time constant is chosen greater than or equal to the AWC sample time. Increasing the AWC sample rate beyond that only gradually decreases the energy gain.

To study the impact of hysteresis on the performance of the dynamic adaptation strategy, the right-hand side plot in Fig. 7 is provided. There the energy gain is expressed against the AWC sample time for a fixed LF filter time constant of 300s. Interestingly, the impact of hysteresis on the energy gain remains relatively small, especially for the sample rates below 2 min. In fact, hysteresis types $\mathscr{H}_{(-1,1)}$ and $\mathscr{H}_{(-2,2)}$ even seem to have a slightly positive impact on the energy gain in this region.

Next, the impact on the yaw system is studied. To this end, only the yaw dynamics of an upstream wind turbine (T7) is considered. The reason for this choice is that the yaw misalignment angles ot this first turbine are larger than the misalignment angles of the downstream turbines, resulting in larger nacelle motions. In this way, the worst case yaw duty will be analysed. In Fig. 8, the yaw duty cycle (left plot) and the number of yaw manoeuvres per hour

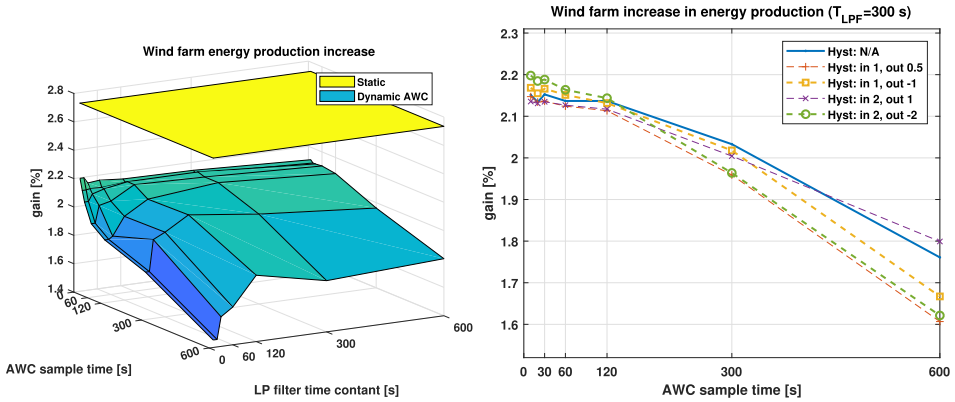

Fig. 7. Energy gain versus the AWC sample time for: (left) different LP filter time constants and hysteresis is not active, and (right) for constant LP filter time constant (300 s) and all considered choices of hysteresis.

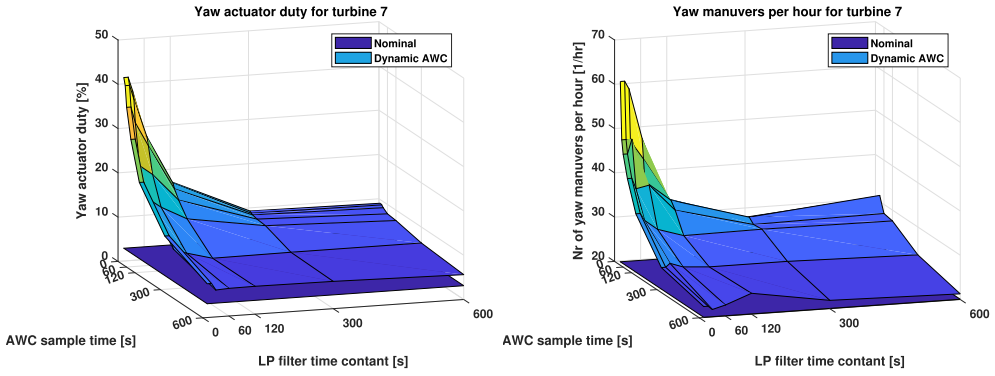

Fig. 8. Yaw duty cycle (left) and number of yaw manoeuvres (right) versus the AWC sample time and LP filter time constant. Hysteresis is not active.

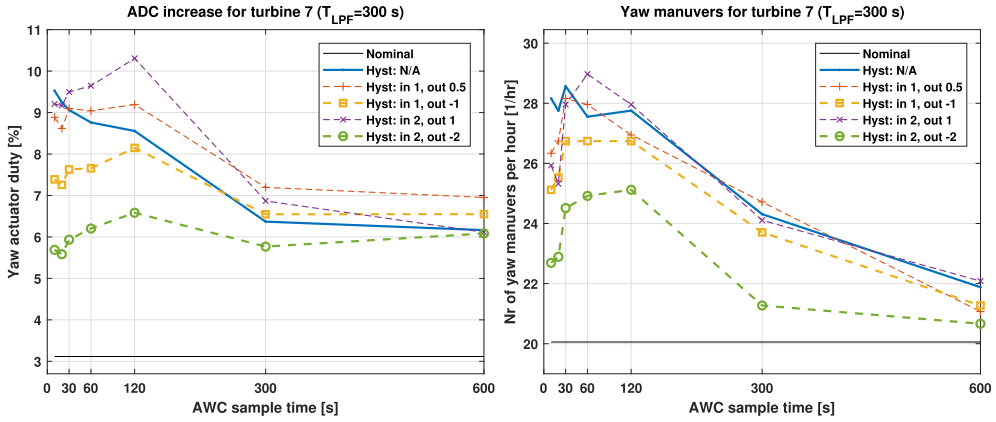

Fig. 9. Yaw duty cycle (left) and number of yaw manoeuvres (right) versus the AWC sample time for the considered choices of hysteresis.

(right plot) are given versus the AWC sample time and LP filter time constant. Hysteresis is not included in these two plots. Clearly, the sensitivity of the yaw duty cycle is much more pronounced than that of the energy gain, especially for the more aggressive adaptation strategies, i.e. for sample times and LP filter time constants below the 2 min. Sample times and time constants above 120 s result in lower levels of yawing. Combined with the conclusions made above related to energy gain, an AWC sample time of 120s in combination with LP filter time constant of 300s seem to give a good balance between energy gain and yaw actuator duty cycle increase.

Adding hysteresis can further reduce the yaw duty and number of manoeuvres. This can be observed from the two plots in Fig. 9, which depict the yaw duty cycle (left) and number of yaw manoeuvres per hour (right) versus the AWC sample time for the considered choices of hysteresis. These plots are for a fixed LP filter time constant of 300s. Clearly, the $\mathscr{H}_{(-2,2)}$ hysteresis delivers best results in terms of loading on the yaw system, which occurs at practically no negative impact on the energy gain (see Fig. 7). Interestingly, the lowest yaw motion occurs for the sample times below 120 s. This may in first instance seem counter-intuitive as one may generally expect increasing the AWC sample rate (or, equivalently, decreasing the sample time) would increase the yaw activity. However, it is the rate of change of the yaw angle *setpoint* that will increase as a consequence of a higher AWC sample rate, and that does not necessarily lead to an actual increase of the nacelle motion (yaw angle). In fact, as Fig. 9 suggests, it is the other way around: when the wind direction changes, with a faster AWC sample rate the yaw setpoint will be adapted faster, which will give rise to a smaller yaw error (difference between the yaw angle and its setpoint) than when the yaw setpoint is kept constant for a longer period of time due to a lower AWC sample rate. Due to that, the yaw motor needs to move less to compensate for the yaw error when the AWC sample rate is faster. As a result of that, best results in terms of yaw duty are achieved at AWC sample times of 10–20s. If required, further reductions of yaw manoeuvres are possible by increasing the AWC sample time, but only at the expense of some energy gain.

4. Conclusions

From the performed analysis it can be concluded that under realistic variations of the wind resource, the dynamic control of the nacelle orientation must be designed carefully to ensure good energy increase at acceptable yaw effort. To achieve that, the yaw misalignment setpoints need to be determined based on dynamically processed wind direction measurements. The results from the sensitivity study performed indicate that well balanced results in terms of energy gain and yaw duty are achieved for AWC sample times below 120 s, provided that the time constant of the LP filter is not smaller than the sample rate. For these parameter ranges, including hysteresis ($\mathscr{H}_{(-2,2)}$) leads to a substantial reduction of the yaw duty at very little (yet, positive) impact on the energy gain. With this hysteresis, an AWC sample time of 20 s, and an LP filter sample time of 300 s, the energy gain from wake redirection (2.19%) is about 20% lower than that based on idealistic static analysis (2.73%), i.e. when one assumes the nacelle can instantly follow the yaw misalignment setpoints resulting from unprocessed wind measurements. For the most upstream wind turbine, the yaw duty cycle increases from around 3.1%–5.6%, and the number of yaw manoeuvres gets about 15% higher. For downstream turbines, the impact on yaw duty is lower due to the smaller yaw misalignment angles these get. Notice also that these results are only representative for conditions similar to those simulated, i.e. when the average wind direction is more or less along the rows of turbines. On annual basis, these percentage increases will, of course, be much less pronounced.

References

[1] G. Corten, P. Schaak, Method and Installation for Extracting Energy from a Flowing Fluid, 2004.
[2] G. Corten, K. Lindenburg, P. Schaak, Assembly of Energy Flow Collectors, Such as Windpark, and Method of Operation, 2004.
[3] G. Corten, P. Schaak, Heat and flux: increase of wind farm production by reduction of the axial induction, in: Proceedings of the European Wind Energy Conference (EWEC), 2003. Madrid, Spain.
[4] K. Boorsma, Active wake control by pitch adjustment. analysis of field measurements, in: Tech. Rep. ECN-E–15-042, Energy research Centre of the Netherlands, 2015.
[5] J. Annoni, P. Gebraad, A. Scholbrock, P. Fleming, J.-W. van Wingerden, Analysis of axial-induction-based wind plant control using an engineering and a high-order wind plant model, Wind Energy 19 (6) (2016) 1135–1150.
[6] F. Campagnolo, V. Petrović, C. Bottasso, A. Croce, Wind tunnel testing of wake control strategies, in: Proceedings of the American Control Conference, 2016. Boston, MA, USA.
[7] P. Fleming, P. Gebraad, S. Lee, J. van Wingerden, K. Johnson, M. Churchfield, J. Michalakes, P. Spalart, P. Moriarty, Simulation comparison of wake mitigation control strategies for a two-turbine case, Wind Energy 18 (12) (2015) 2135–2143.
[8] P. Gebraad, F. Teeuwisse, J. van Wingerden, P. Fleming, S. Ruben, J. Marden, L. Pao, Wind plant power optimization through yaw control using a parametric model for wake effects - a CFD simulation study, Wind Energy 19 (1) (2014) 95–114.
[9] P. Fleming, A. Ning, P. Gebraad, K. Dykes, Wind plant system engineering through optimization of layout and yaw control, Wind Energy 19 (2) (2016) 329–344.
[10] C.R. Shapiro, D.F. Gayme, C. Meneveau, Modelling yawed wind turbine wakes: a lifting line approach, J. Fluid Mech. 841 (2018).

[11] M. Bastankhah, F. Porté-Agel, Experimental and theoretical study of wind turbine wakes in yawed conditions, J. Fluid Mech. 806 (2016) 506–541.
[12] M. van Dijk, J.-W. van Wingerden, T. Ashuri, Y. Li, Wind farm multi-objective wake redirection for optimizing power production and loads, Energy 121 (2017) 561–569.
[13] S. Kanev, F. Savenije, W. Engels, Active wake control: an approach to optimize the lifetime operation of wind farms, Wind Energy 21 (2018) 448–501.
[14] S. Raach, S. Boersma, J.-W. van Wingerden, D. Schlipf, P.W. Cheng, Robust lidar-based closed-loop wake redirection for wind farm control, Proc. IFAC World Congr. 50 (1) (2017) 4498–4503, 2017.
[15] P. Fleming, J. Annoni, J.J. Shah, L. Wang, S. Ananthan, Z. Zhang, K. Hutchings, P. Wang, W. Chen, L. Chen, Field test of wake steering at an offshore wind farm, Wind Energy Sci. 2 (2017) 229–239.
[16] P. Gebraad, F. Teeuwisse, J. van Wingerden, P. Fleming, S. Ruben, J. Marden, L. Pao, A data-driven model for wind plant power optimization by yaw control, in: Proceedings of the American Control Conference, 2014.
[17] P. Fleming, P. Gebraad, S. Lee, J. van Wingerden, K. Johnson, M. Churchfield, J. Michalakes, P. Spalart, P. Moriarty, High-fidelity simulation comparion of wake mitigation control strategies for a two-turbine case, in: ICOWES2013 Conference, Lyngby, 2013.
[18] C. Bak, F. Zahle, R. Bitsche, T. Kim, A. Yde, L.C. Henriksen, A. Natarajan, M. Hansen, Description of the dtu 10 mw reference wind turbine, in: Tech. Rep. DTU Wind Energy Report-I-0092, DTU Wind Energy, Jun. 2013.
[19] H. Özdemir, E. Bot, An advanced method for wind turbine wake modeling, in: Proceedings of the AIAA SciTech Forum, 2018.
[20] E. Bot, FarmFlow validation against full scale wind farms, in: Tech. Rep. ECN-E–15-045, Energy research Centre of the Netherlands, 2015.